http://dx.doi.org/10.14500/aro.11978

Influence of Tetramethylammonium Hydroxide Cation Concentration on Omega Zeolite Crystal Size

Muwafaq M. Yahya[1†], Rana T. AL-Rubaye[1] and Aqeel A. Al-Ani[2]

[1]Department of Chemical Engineering, Faculty of Engineering, Baghdad University, Baghdad – F.R. Iraq

[2]Ministry of Oil, Oil Marketing Company (SOMO) Baghdad, Baghdad – F.R. Iraq

***Abstract*—Omega zeolite nanocrystals can be synthesized hydrothermally from a sodium aluminosilicate solution characterized by a 5.96 Na_2O/Al_2O_3 constant molar ratio, carried out at a maximum temperature of about 100°C for 4 days after aging at room temperature for 3 days, utilizing tetramethylammonium hydroxide (TMA-OH) at molar ratios of 0.36, 0.48, and 0.61. By using different analysis techniques, such as X-ray diffraction, energy-dispersive X-ray spectroscopy, scanning electron microscopy, and atomic force microscopy, the physical characteristics of the nanosized omega zeolite crystals can be identified, and the omega zeolite crystal size can be regulated between 34 and 100 nm. In this research paper, the process of creating a uniform aluminosilicate solution with TMA-OH, followed by forming a solid aluminosilicate gel with adjusted elemental composition, reveals the significance of the TMA-OH/Al_2O_3 mole ratio for synthesizing nanocrystalline omega zeolite aggregates.**

***Index Terms* – Nanocrystal, Omega zeolite, Sodium-aluminosilicate, Tetramethylammonium hydroxide.**

I. Introduction

Discovered in 1972 within the basalt lava of Mont-Sémiole, "near Montbrison," France, the Omega synthetic aluminosilicate zeolite is one of several types of zeolite, including ZSM-4 (Galli, et al., 1974), and LZ-202 (Breck and Skeels, 1985) that own the Mazzite framework, which is naturally occurring zeolite. Furthermore, this zeolite framework contains a 12-membered ring pore found by (Galli, et al., 1974) and (Rinaldi, Pluth and Smith, 1975) and has garnered significant research interest due to its notable Brønsted acidity and catalytic capabilities in processes such as alkylation (Flanigen and Kellberg, 1980), cracking (Báfero, et al., 2020), and isomerization (Mahdi and Muraza, 2016).

ARO-The Scientific Journal of Koya University
Vol. XIII, No. 1 (2025), Article ID: ARO.11978. 7 pages
DOI: 10.14500/aro.11978
Received: 29 December 2024; Accepted: 20 March 2025
Regular research paper; Published: 31 March 2025
†Corresponding author's e-mail: muwafaq.yahya1507d@coeng.uobaghdad.edu.iq

Numerous patents and scholarly articles detail the synthetic counterpart of mazzite (omega zeolite), which typically forms at low temperatures (approximately 353–423 K) within the (tetramethylammonium hydroxide [TMA-OH])–NaOH–Al_2O_3–SiO_2–H_2O system (Feng, et al., 2020; Martucci, et al., 2003; Goossens, et al., 2000; McQueen, et al., 1994). Across this process, TMA-OH serves as a structure-directing agent (SDA), while other organic compounds, including pyrrolidine (Flanigen and Kellberg, 1980), piperazine (Xu, et al., 2007), glycerol (Yang and Evmiridis, 1994), and p-dioxane (De Witte, et al., 1997), have also been utilized as templating agents. In the past 30 years, there has been much awareness of the use of organic molecules as SDAs in the texture synthesis of aluminosilicate zeolites (Shi, et al., 2012). In the middle process of preparation of omega zeolite, TMA cations may become trapped in gmelinite cages during crystal growth, which is assumed to be a strong structure-directing factor (Feng, et al., 2020; Martucci, et al., 2003; Goossens, et al., 2000). A vast range of morphologies has been documented for omega zeolites, such as euhedral crystals in the shape of hexagonal prisms, barrels, spheres, or rosettes, in uneven forms such as bundles or needles (Araya, et al., 1984; Fajula, et al., 1989; DiRenzo, et al., 1994; Edmunds, et al., 1989). The aluminum concentration could be the key to the crystal morphology in the synthesis mixture (Goossens, et al., 2000; McQueen, et al., 1994), or when using an alcohol medium during the reaction mixture, the alcohol type and its ratio inside the water may play a significant role also (Gies and Marker, 1992). Some findings indicate that SDAs function not merely as pore fillers but, with the assistance of van der Waals forces, mainly interact with the Si species inside the zeolite (Gómez-Hortigüela, et al., 2004). The final crystalline structure geometry of zeolite pores and the type of final crystalline structure are influenced by SDAs. The concentration of the organic template in the zeolite framework can be affected by the interaction type between zeolite pre-cursors and SDAs (Gómez-Hortigüela, et al., 2004; Sastre, et al., 2003). Furthermore, the structures formed during the crystallization of zeolites by employing SDAs are probably not the stabilized ones but those with the greatest nucleation abilities, developing under either thermodynamic or kinetic control. This occurrence depends on the conditions

of the crystals' growth step during the crystallization operation (Tosheva and Valtchev, 2005). The existence of Na+ cations is necessary to achieve the charge balance in the route of the crystal growth because the TMA cations are not adequate to balance the entire charge of the anionic lattice. Based on all previous facts, it can be said that the MAZ-type zeolites essentially depend on TMA in the figuration of its establishment (McQueen, et al., 1994).

II. Preparation

The reagents used were TMA-OH (25% solution in water) from MERCK (UN 1835) used as a template, sodium hydroxide (NaOH, >99.0 wt%), and distilled water. Sodium aluminate (density 2.6 g/cm^3, molecular weight = 81.97 g/mol.) (50–60% Al_2O_3, ≤0.05% Fe_2O_3, 37–45%Na_2O) and silica colloidal HS-40 (40 wt. % suspension in H_2O) bought from Sigma Aldrich (MERCK). A typical gel sample was prepared in the laboratories of the chemical engineering department at Baghdad University for about 7 days. First, the gel is prepared by mixing NaOH, H_2O, TMA-OH, and $NaAlO_2$ in an appropriate plastic beaker at room temperature for 30 min. The silica sol was added drop by drop with stirring until homogeneity occurred. After further mixing for 30 min, the mixture was kept inside a 125 mL stainless Teflon-lined steel autoclave, aged statically for three days at a temperature of about 25°C, and after that stored in an oven for 4 days at 100°C. The solid product was washed with deionized water until the pH of the residue water reached about 7–8, and then dried overnight at 100°C.

TABLE I
Batch Requirement for Omega Zeolite Synthesis

Material	Run 1 (Moles)	Molar Ratio	Run 2 (Moles)	Molar Ratio	Run 3 (Moles)	Molar Ratio
Al_20_3	0.0160	1.00	0.0160	1.00	0.0160	1.00
NaOH	0.0957	5.98	0.0957	5.98	0.0957	5.98
TMA-OH	0.0057	0.36	0.0077	0.48	0.0098	0.61
H_2O	1.7837	111.4	1.8147	113.3	1.8478	115.4
SiO_2	0.1605	10.02	0.1605	10.02	0.1605	10.02

Al_2O_3=Aluminum oxide, NaOH=Sodium oxide, TMA-OH=Tetramethylammonium-hydroxide, H_2O=Water molecule, SiO_2=Silicon dioxide

Table I shows the batch requirement for omega synthesis with varied TMA-OH/Al_2O_3 mole ratios of about 0.36, 0.48, and 0.61. The X-ray diffractometry (XRD) analysis on the ADX2700 SSC (30 mA, 40 kV) device was used to specify the crystallinity, phase lucidity, and stratification of the acquired samples. The crystal morphology and crystal size were determined by scanning electron microscopy (SEM) (Quattro–STEM/SEM) Thermo Fisher Scientific (X2500000, 0.8 nm, 5-axis). The carbon, oxygen, and sodium (Na) weight percent and the silica/alumina bulk ratio were specified on energy dispersive X-ray spectroscopy (EDXS) detectors, in addition to atomic force microscopy (AFM) (CoreAFM) analysis to show the surface morphology differences between the omega zeolite samples.

III. Results and Discussion

The XRD patterns of Omega zeolite samples from experiments Run 1, Run 2, and Run 3 using CuKα radiation are illustrated in Fig. 1a-c, respectively. The first sight may show that the zeolite omega is an "intermediate phase" crystallizing in the interfering crystallization fields of ZSM-4 zeolite (Mahdi and Muraza, 2016), and the ZSM-34 zeolite (Wu, et al., 2008), which proved that TMA-OH plays a structure-directing role with Na+ (sodium cation) in the formation of zeolite omega.

Table II shows the extended report of the XRD peak ID, the report shows 2-theta for standard and typical samples of Runs 1, 2, and 3, along with the crystal size and delta size for typical samples only. The data for all samples, when compared with data announced in the literature on crystal size for (Perrotta, et al., 1978), show almost identical results to those of omega zeolite in the case of the stances and some differences in relative intensities of the diffraction peaks. The sample from Run 1, where the mole ratio of TMA-OH/Al_2O_3 is about 0.36, shows a maximum crystal size of not more than 48 nm and a delta of not <0.052, while the sample from Run 3 with a TMA-OH/Al_2O_3 mole ratio of about 0.61 shows crystal size values of more than 100 nm at several points and a delta value of not <0.041. The maximum crystal size for Omega zeolite can obtained when the mole

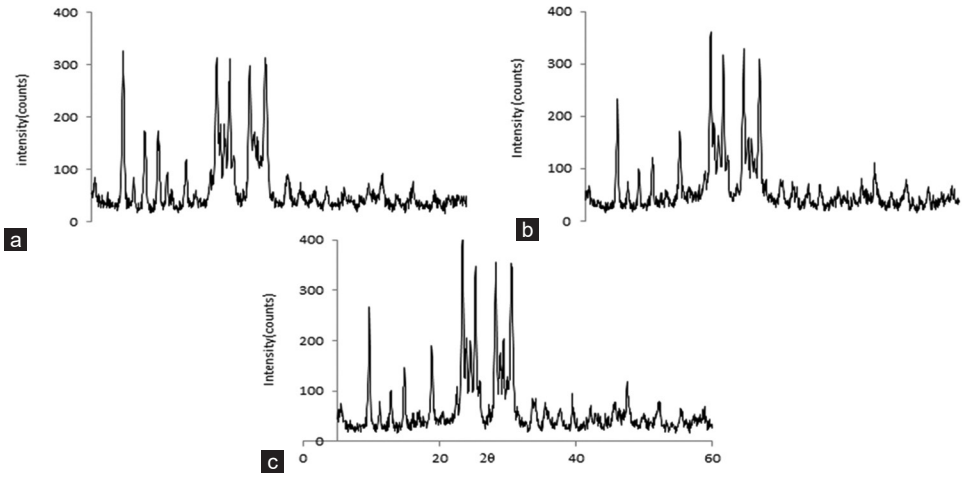

Fig. 1. XRD patterns of samples of Run 1 (a), Run 2 (b), and Run 3 (c) using CuKα radiation.

 http://dx.doi.org/10.14500/aro.11978

TABLE II
THE EXTENDED REPORT OF THE XRD PEAK ID, THE REPORT SHOWS 2-THETA FOR STANDARD AND TYPICAL SAMPLES OF RUNS 1, 2, AND 3

2-Theta*	Run 1			Run 2			Run 3		
	2-Theta	Delta	Crystal size (nm)	2-Theta	Delta	Crystal size (nm)	2-Theta	Delta	Crystal size (nm)
5.589	5.377	0.212	48	-	-	-	5.46	0.129	>100
9.744	9.558	0.185	31	9.722	0.022	60	9.667	0.076	57
11.248	11.092	0.156	33	11.275	−0.027	>100	11.199	0.049	61
12.894	12.761	0.133	24	12.897	−0.003	93	12.854	0.041	48
14.902	14.744	0.158	29	14.891	0.011	43	14.838	0.064	41
16.19	16.033	0.157	21				16.12	0.07	>100
16.939	16.647	0.292	21	16.974	−0.035	25	16.874	0.065	36
18.988	18.809	0.179	27	18.927	0.061	28	18.863	0.125	32
20.352	20.196	0.155	46	-	-	-	-	-	-
22.665	22.553	0.112	31	-	-	-	22.575	0.09	>100
23.516	23.332	0.183	14	23.484	0.032	22	23.394	0.122	26
24.098	-	-	-	23.95	0.148	18	23.863	0.235	26
24.71	24.505	0.205	16	24.623	0.087	15	24.546	0.163	26
25.427	25.227	0.2	14	25.332	0.096	16	25.252	0.175	23
26.033	25.85	0.183	22	25.79	0.242	26	25.768	0.265	30
27.334							27.317	0.017	82
28.401	28.204	0.197	14	28.312	0.088	19	28.246	0.154	28
28.966	28.85	0.116	7	28.877	0.089	16	28.905	0.061	16
29.709	-	-	-	29.503	0.052	22	29.361	0.193	25
30.742	30.483	0.259	15	30.644	0.098	29	30.569	0.173	19
33.862	33.774	0.088	15	33.82	0.042	16	33.807	0.056	15
35.655	35.603	0.052	29	35.627	0.028	21	35.579	0.076	17
37.949	37.673	0.277	16	37.804	0.145	17	37.665	0.285	17
39.709	39.451	0.258	29	39.627	0.081	25	39.556	0.152	45
42.318	42.081	0.237	21	42.25	0.068	47	42.161	0.157	>100
45.935	45.671	0.265	20	45.726	0.21	34	45.7	0.235	17
47.78	47.592	0.188	21	47.643	0.137	30	47.59	0.191	27

ratio of TMA-OH/Al_2O_3 is about 0.48, where crystal size ranges from 20 to more than 100 nm with a minimum delta reaching a negative value of about −0.027. Fig. 2 shows a histogram chart comparison and differences in crystal size between these samples. By comparing the delta value, which represents the differences between the prepared samples and the memory background inside the XRD device, it was found that the zeolite with the smallest delta value was the best match for the pure form of zeolite omega.

The effect of the mole ratio of TMA-OH/Al_2O_3 on particle size growth can be seen in Fig. 3, which represents SEM analysis images of omega zeolite samples for Run 1, Run 2, and Run 3, respectively. These figures clearly show how the crystals appear at different concentrations of organic structure directing agent (OSDA). At low concentrations, there are intercrystallite voids of about 10 μm and an irregular particle size between 36 nm and 117 nm; these voids become narrower and the crystallinity grows to a uniform size between 60 and 70 nm after reaching a concentration of 0.48. When the concentration becomes about 0.61, there is an expansion of the distance between the crystals, which become rod-like and have an apparent size between 43 nm and 93 nm due to scattering as a result of increased polarization by OSDA.

The AFM analysis includes a mean diameter histogram chart, 2D particle analysis, 3D view of the surface, and the mean magnitudes of particle diameter, area, and Z-maximum. Figs. 4 and 5 show the average particle diameter, area, and

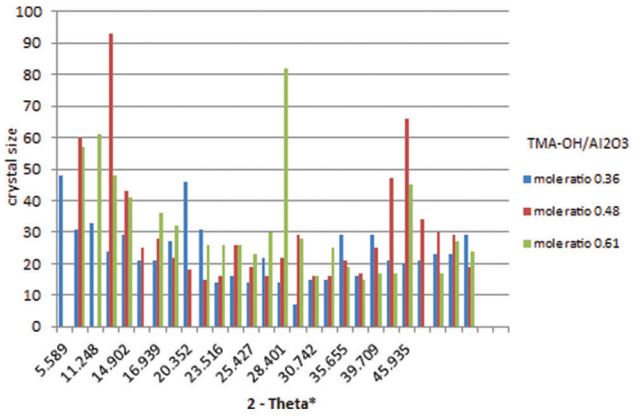

Fig. 2. Histogram chart comparison and differences between crystal size omega zeolite samples from Run 1, 2, and Run 3.

Z-max for both samples from Run 1 and Run 3, which were about 36 nm, 41 nm, and 2659 nm^2 and 38 nm, 265 nm, and 2786 nm^2, respectively, with incomplete or distorted crystallization in Fig. 4, and inhomogeneous distribution of particles after disintegration to a smaller diameter on the surface in Fig. 5, while Fig. 6 shows an almost uniform spread of complete particle crystallization with an average diameter of about 95 nm, an average Z-max of about 252 nm, and an average area of about 14608 nm^2. Thus, with a stable Na_2O/Al_2O_3 ratio in the range (6.0–8.0) required for the preparation of mazzite (omega zeolite), the added appropriate

amount of TMA-OH was clearly presented as a strong SDA in the synthesis of omega zeolite (Dwyer and Chu, 1979).

Finally, Figs. 7-9 show the EDS analysis of omega zeolite samples from Run 1, Run 2, and Run 3 as peaks for the main components of omega zeolite, and the results are inserted in Table III. The results show that the maximum carbon weight percent occupying was about 12% by omega zeolite with a TMA-OH/Al_2O_3 mole ratio of about 0.48, and it is more than the rest samples, this is due to the good and high crystallization during preparation. The Si/Al bulk ratio was about 3.037, 3.07, and 3.5, respectively, with a fixed mixed Na_2O/Al_2O_3 mole ratio of about 5.96.

The status here is proportionate with preceding arguments (Brady and Walther, 1990; Pinar, et al., 2007) regarding cooperative structure directing effects in high or low silica zeolites using a collection of macro- and microstructure directing agents (Dove and Crerar, 1990; AL-Rubaye and Garforth, 2018; Najwa and and Asir, 2015; Abd Al-Rubaye, 2017). The organization of TO^4 tetrahedral units by TMA-OH molecules may not be strongly adequate, leading to the formation of amorphous materials. However, small Na+ ions existing in the synthesis gel can develop the crystallization process by helping to conquer the energy barrier of nucleation (Hussam and Hussein, 2019; Al-Rubaye, 2013; Najwa and Asir, 2016). At the same time, Na+ affects the types of secondary building blocks established in the gel, leading to the formalization of various zeolites (Rallan, Al-Rubaye and Garforth, 2015; Ammar and Sally, 2017). However, with the addition of TMA-OH, these small inorganic existences can progressively aggregate around TMA-OH, opening

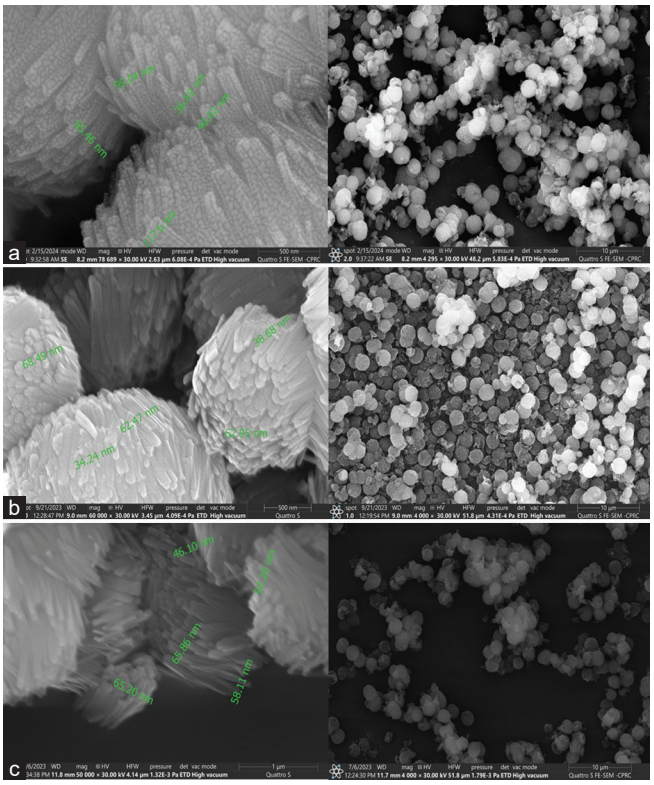

Fig. 3. Scanning electron microscopy images of omega zeolite samples from Run 1 (a), Run 2 (b), and Run 3 (c).

TABLE III
WEIGHT PERCENT OF SILICON, ALUMINUM, AND SODIUM OF PREPARED OMEGA ZEOLITE FROM RUN 1, 2, AND RUN 3

Zeolite type/ Element	Na-omega Tma-oh/al_2o_3 Molar ratio 0.36 Run 1	Na-omega Tma-oh/al_2o_3 Molar ratio 0.48 Run 2	Na-omega Tma-oh/al_2o_3 Molar ratio 0.61 Run 3
	Weight %	Weight %	Weight %
C	5.8	12.0	3.6
O	54.8	51.8	48.3
Na	6.9	6.2	5.9
Al	7.9	6.8	9.4
Si	24.0	20.9	32.9
Ca	0.6	0.0	0.0
Cu	0.0	2.3	0.0

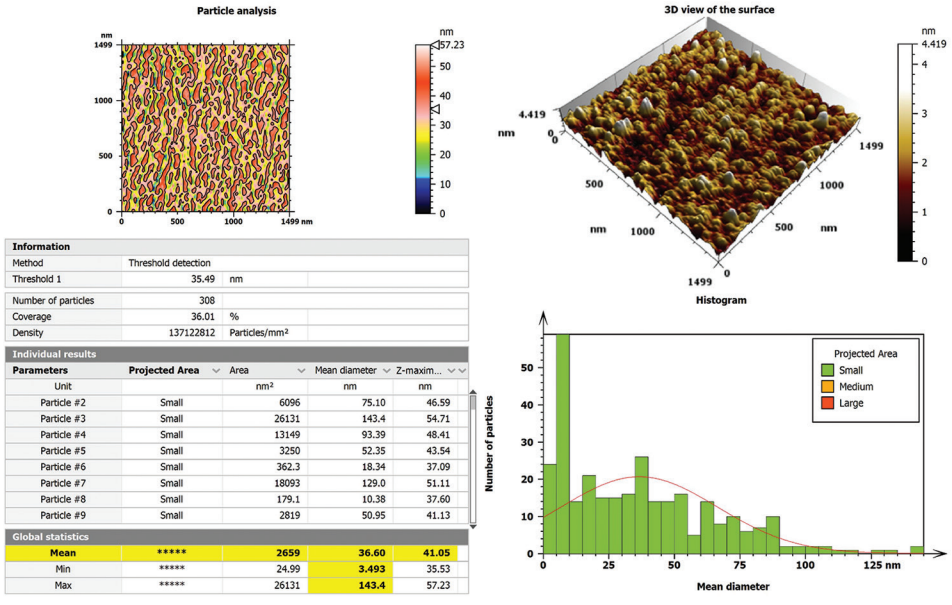

Fig. 4. Atomic force microscopy analysis of omega zeolite sample from Run 1.

http://dx.doi.org/10.14500/aro.11978

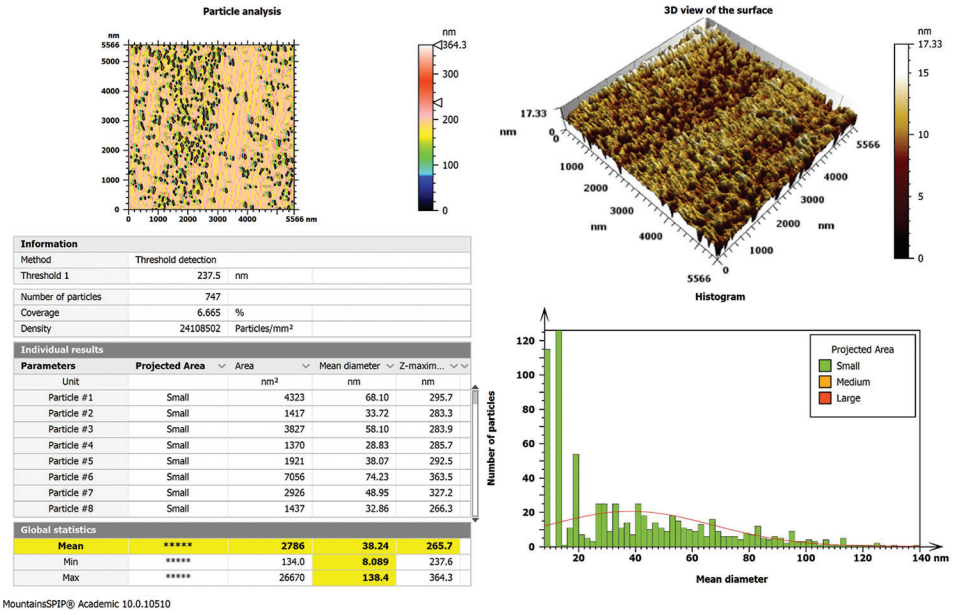

Information		
Method	Threshold detection	
Threshold 1	237.5	nm
Number of particles	747	
Coverage	6.665	%
Density	24108502	Particles/mm²

Individual results				
Parameters	Projected Area	Area	Mean diameter	Z-maxim...
Unit		nm²	nm	nm
Particle #1	Small	4323	68.10	295.7
Particle #2	Small	1417	33.72	283.3
Particle #3	Small	3827	58.10	283.9
Particle #4	Small	1370	28.83	285.7
Particle #5	Small	1921	38.07	292.5
Particle #6	Small	7056	74.23	363.5
Particle #7	Small	2926	48.95	327.2
Particle #8	Small	1437	32.86	266.3
Global statistics				
Mean	*****	**2786**	**38.24**	**265.7**
Min	*****	134.0	**8.089**	237.6
Max	*****	26670	**138.4**	364.3

Fig. 5. Atomic force microscopy analysis of omega zeolite sample from Run 3.

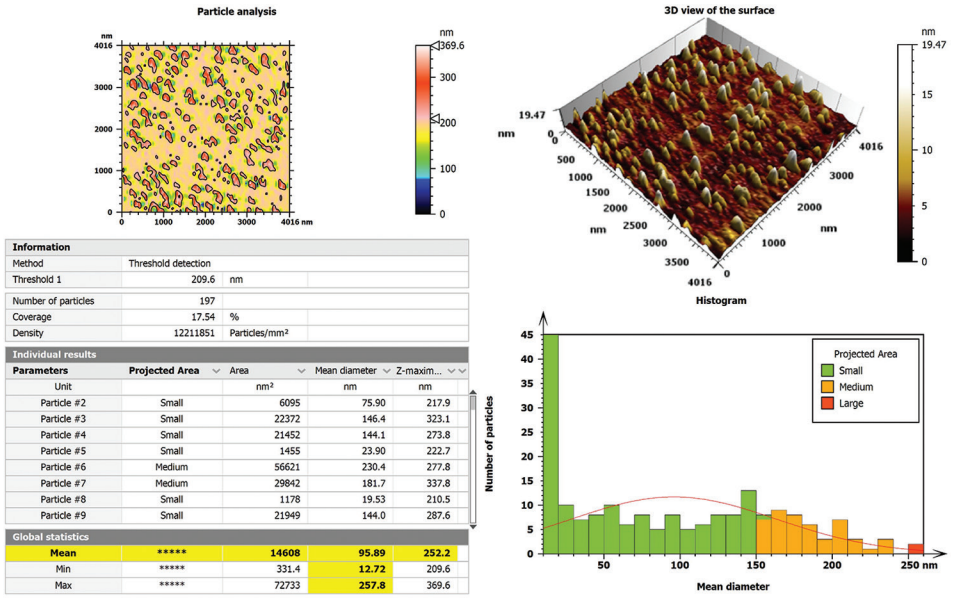

Information		
Method	Threshold detection	
Threshold 1	209.6	nm
Number of particles	197	
Coverage	17.54	%
Density	12211851	Particles/mm²

Individual results				
Parameters	Projected Area	Area	Mean diameter	Z-maxim...
Unit		nm²	nm	nm
Particle #2	Small	6095	75.90	217.9
Particle #3	Small	22372	146.4	323.1
Particle #4	Small	21452	144.1	273.8
Particle #5	Small	1455	23.90	222.7
Particle #6	Medium	56621	230.4	277.8
Particle #7	Medium	29842	181.7	337.8
Particle #8	Small	1178	19.53	210.5
Particle #9	Small	21949	144.0	287.6
Global statistics				
Mean	*****	**14608**	**95.89**	**252.2**
Min	*****	331.4	**12.72**	209.6
Max	*****	72733	**257.8**	369.6

Fig. 6. Atomic force microscopy analysis of omega zeolite sample from Run 2.

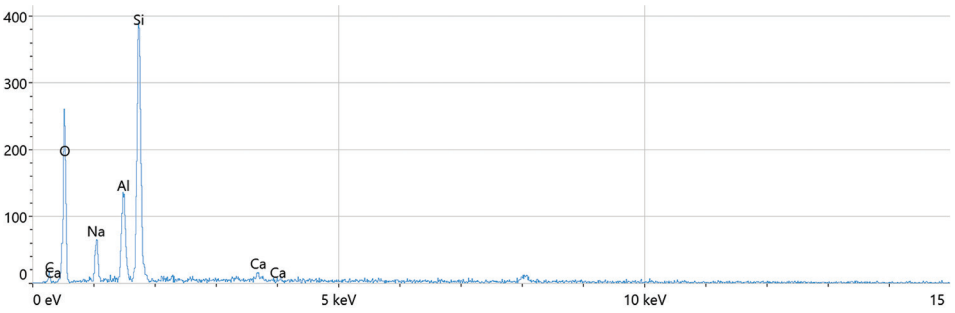

Fig. 7. EDXA analysis of Run 1 mega zeolite samples.

up the chance of omega zeolite crystallization. Synthesis data showed that Na+ and the exact weight of TMA-OH may have a cooperative structure-directing effect on the preparation of pure zeolite omega (Martucci, et al., 2003).

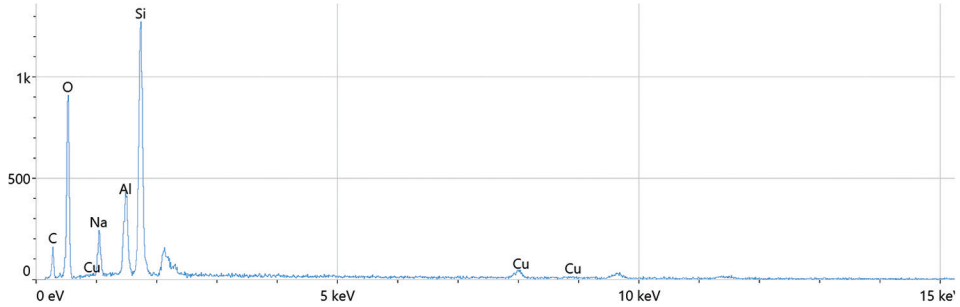

Fig. 8. EDXA analysis of Run 2 omega zeolite samples.

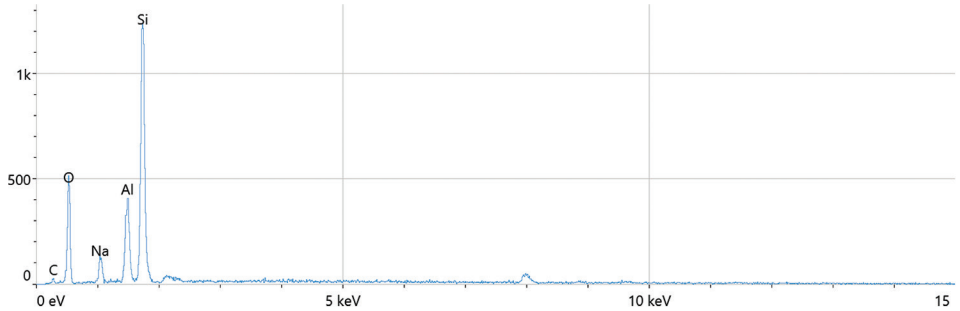

Fig. 9. EDXA analysis of Run 2 omega zeolite samples.

IV. Conclusion

The synthesis of zeolites using clear primary solutions and colloidal suspensions, which are stable materials, is one of the most efficient and widely used techniques. The omega zeolite has been effectively synthesized hydrothermally from a sodium aluminosilicate-TMA-OH solution at a fixed Na_2O/Al_2O_3 mole ratio of about 5.96 and a maximum temperature of around 100°C with aging and crystallization time within 7 days. The High purity, good crystallinity, and uniform morphology of the omega zeolite sample can be obtained when the TMA-OH/Al_2O_3 mole ratio is almost 0.48 with a crystal size of about 95 nm, a mean particle diameter of about 93 nm, a mean Z-maximum of almost 252 nm, and a mean surface area of about 14608 nm². The organic templates may play an important role in the stability of zeolite omega and deserve some attention. It has been observed that the preparation of pure omega zeolite requires a precise amount of TMA-OH to be used.

References

Abd Al-Rubaye, R.T., 2017. Influence Factors on zeolite Y Crystal growth. *Sigma*, 17, p.18.

Al-Rubaye, R., 2013. G*eneration and Characterisation of Catalytic Films of Zeolite Y and ZSM-5 on FeCrAlloy Metal.* The University of Manchester, United Kingdom.

AL-Rubaye, R.T.A., and Garforth, A.A., 2018. Study the effect of various parameters on the synthesis of ZSM-5 zeolite. *Journal of Engineering*, 24(11), pp.30-40.

Ammar, S.A., and Sally, A.H., 2017. Equilibrium, kinetic and thermodynamic study of aniline adsorption over prepared ZSM-5 Zeolite. *Iraqi Journal of Chemical and Petroleum Engineering*, 18(1), pp.47-56.

Araya, A., Barber, T.J., Lowe, B.M., Sinclair, D.M., and Varma, A., 1984. The synthesis and thermal behaviour of zeolite Ω. *Zeolites*, 4(3), pp.63-269.

Báfero, G.B., Araújo, V.A., Almeida, R.K.S., and Pastore, H.O., 2020. Catalytic performance of ferrierite and omega zeolites obtained through 2D-3D-3D transformation from Na-RUB-18 layered silicate. *Microporous and Mesoporous Materials*, 302, p.110216.

Brady, P.V., and Walther, J.V., 1990. Kinetics of quartz dissolution at low temperatures. C*hemical Geology*, 82(C), pp.253-264.

Breck, D.W., and Skeels, G.W., 1985. *Silicon Substituted Zeolite Compositions and Process for Preparing Same*. In US Patent 4,503,023.

De Witte, B., Patarin, J., Guth, J.L., and Cholley, T., 1997. Synthesis of mazzite-type zeolites in the presence of organic solvents: Study of the structure directing role of p-dioxane. *Microporous Materials*, 10(4-6), pp.247-257.

DiRenzo, F., Fajula, F., Figueras, F., Nicolas, S., and Couriers, T., 1989. Are the general laws of crystal growth applicable to zeolite synthesis? *Studies in Surface Science and Catalysis*, 49(C), pp.119-132.

Dove, P.M., and Crerar, D.A., 1990. Kinetics of quartz dissolution in electrolyte solutions using a hydrothermal mixed flow reactor. *Geochimica et Cosmochimica Acta*, 54(4), pp.955-969.

Dwyer, F.G., and Chu, P., 1979. ZSM-4 crystallization via faujasite metamorphosis. *Journal of Catalysis*, 59(2), pp.263-271.

Edmunds, M.P.W., Hill, S.J., Latham, K., and Williams, C.D., 1994. Synthesis of zeolite omega in an alcohol-water system. *Zeolites*, 14(7), p.529-532.

Fajula, F., Nicolas, S., Di Renzo, F., Figueras, F., and Gueguen, C., 1989. In: *Zeolite Synthesis, ACS Symposium*. Vol. 398. American Chemical Society, Washington, DC, p.493.

Feng, Z., Wang, Y., Lv, T., Zhang, S., Liu, X., Liu, X., and Meng, C., 2020. Hydrothermal conversion of kenyaite into zeolite omega in tetramethylammonium cations system. *Solid State Sciences*, 103, p.106196.

Flanigen, E.M., and Kellberg, E.R., 1980. *Synthetic Crystalline Zeolite and Process for Preparing Same*. In US Patent No. 4241036.

Galli, E., Passaglia, E., Pongiluppi, D., and Rinaldi, R., 1974. Mazzite, a new mineral, the natural counterpart of the synthetic zeolite Ω. *Contributions to Mineralogy and Petrology*, 45(2), pp.99-105.

Gies, H., and Marker, B., 1992. The structure-controlling role of organic templates for the synthesis of porosils in the systemsSiO_2/template/H_2O. *Zeolites*, 12(1), pp.42-49.

Gómez-Hortigüela, L., Corà, F., Catlow, C.R.A., and Pérez-Pariente, J., 2004. Computational study of the structure-directing effect of benzylpyrrolidine and its fluorinated derivatives in the synthesis of the aluminophosphate AlPO-5. *Journal of the American Chemical Society*, 126(38), pp.12097-12102.

Goossens, A.M., Feijen, E.J.P., Verhoeven, G., Wouters, B.H., Grobet, P.J., Jacobs, P.A., and Martens, J.A., 2000. Crystallization of MAZ-type zeolites using tetramethylammonium, sodium and n-hexane derivatives as structure-and composition-directing agents. *Microporous and Mesoporous Materials*, 35, pp.555-572.

Hussam, J.M., and Hussein, Q.H., 2019. Synthesis and characterization of Nano Y Zeolite using MWCNT as media for crystal growth. *Iraqi Journal of Chemical and Petroleum Engineering*, 20(4), pp.49-54.

Mahdi, H.I., and Muraza, O., 2016. Conversion of isobutylene to octane-booster compounds after methyl tert-butyl ether phaseout: The role of heterogeneous catalysis. *Industrial and Engineering Chemistry Research*, 55(43), pp.11193-11210.

Martucci, A., Alberti, A., De Lourdes Guzman-Castillo, M., Di Renzo, F., and Fajula, F., 2003. Crystal structure of zeolite omega, the synthetic counterpart of the natural zeolite mazzite. *Microporous and Mesoporous Materials*, 63(1-3), pp.33-42.

McQueen, D., Fajula, F., Dutartre, R., Rees, L.V.C., and Schulz, P., 1994. Diffusion of xylene isomers in dealuminated mazzite zeolites by the frequency response technique. *Studies in Surface Science and Catalysis*, 84(C), pp.1339-1346.

Najwa, S.M., and Asir, A.A., 2015. Synthesis and characterization of nano-crystalline ZSM-5 zeolite. *Al-Khwarizmi Engineering Journal*, 11(4), pp.8-19.

Najwa, S.M., and Asir, A.S., 2016. Synthesis and characterization of nanocrystalline micro-mesoporous ZSM 5/MCM-41 composite zeolite. *Iraqi Journal of Chemical and Petroleum Engineering*, 17(1), pp.71-82.

Perrotta, A.J., Kibby, C., Mitchell, B.R., and Tucci E.R., 1978. The synthesis, characterization, and catalytic activity of omega and ZSM-4 zeolites. *Journal of Catalysis*, 55(2), pp.240-249.

Pinar, A.B., García, R., Arranz, M., and Pérez-Pariente, J., 2007. Co-directing role of template mixtures in zeolite synthesis. *Studies in Surface Science and Catalysis*, 170, pp.383-388.

Rallan, C., Al-Rubaye, R., and Garforth, A., 2015. Generation of catalytic films of alumina and zeolites on FeCrAlloy rods. *Chemical Engineering Transactions*, 43, pp.907-912.

Rinaldi, R., Pluth, J.J., and Smith, J.V., 1975. Crystal structure of mazzite dehydrated at 600°C. *Acta Crystallographica Section B Structural Crystallography and Crystal Chemistry*, 31(6), pp.1603-1608.

Sastre, G., Leiva, S., Sabater, M.J., Gimenez, I., Rey, F., Valencia, S., and Corma, A., 2003. Computational and experimental approach to the role of structure-directing agents in the synthesis of zeolites: The case of cyclohexyl alkyl pyrrolidinium salts in the synthesis of β, EU-1, ZSM-11, and ZSM-12 zeolites. *Journal of Physical Chemistry B*, 107(23), pp.5432-5440.

Shi, Q., Yu, J., Song, Z., and Kang, X., 2012. Cooperative structure-directing effects in the synthesis of a high-silica zeolite mazzite analogue. *Materials Sciences and Applications*, 3(5), pp.306-309.

Tosheva, L., and Valtchev, V.P., 2005. Nanozeolites: Synthesis, crystallization mechanism, and applications. *Chemistry of Materials*, 17(10), pp.2494-2513.

Wu, Z., Song, J., Ji, Y., Ren, L., and Xiao, F.S., 2008. Organic template-free synthesis of ZSM-34 zeolite from an assistance of zeolite L seeds solution. *Chemistry of Materials*, 20(2), pp.357-359.

Xu, H., Dong, P., Liu, L., Wang, J.G., Deng, F., and Dong, J.X., 2007. Synthesis and characterization of zeolite MAZ in Na_2O-Al_2O_3-SiO_2-piperazine-H_2O. *Journal of Porous Materials*, 14(1), pp.97-101.

Yang, S., and Amiridis, N.P., 1994. Synthesis of omega zeolite without use of tetramethylammonium(tma) ions. *Studies in Surface Science and Catalysis*, 84(C), pp.155-162.